

REFERENCE 103

S .R. BIERMAN, E. D. CLAYTON, AND L .E. HANSEN, "CRITICAL EXPERIMENTS WITH HOMOGENEOUS MIXTURES OF PLUTONIUM AND URANIUM OXIDES CONTAINING 8, 15, AND 30 WT% PLUTONIUM," NUCL. SCI. ENG. 50: 115-126 (1973).

NUCLEAR SCIENCE and ENGINEERING®

A JOURNAL OF THE AMERICAN NUCLEAR SOCIETY

EDITOR

DIXON CALLIHAN, *Union Carbide Corporation, Nuclear Division,
Oak Ridge Y-12 Plant
Oak Ridge, Tennessee 37830*

NSENAO 50 (2) 91-184 (1973)

VOLUME 50, NUMBER 2, FEBRUARY 1973

Copyright © 1973 by American Nuclear Society, Inc., Hinsdale, Illinois 60521

Critical Experiments with Homogeneous Mixtures of Plutonium and Uranium Oxides Containing 8, 15, and 30 wt% Plutonium

S. R. Bierman, E. D. Clayton, and L. E. Hansen

Battelle, Pacific Northwest Laboratory, Richland, Washington 99352

Received May 30, 1972

Revised July 31, 1972

Data are presented from critical experiments with mixed $\text{PuO}_2\text{-UO}_2$ fuels containing 30.0, 14.62, and 7.89 wt% Pu and having H/X (H:Pu+U) atomic ratios of 47.4, 30.6, and 51.8, respectively. In addition to the experimental results, which can be used directly as integral benchmark checkpoints, derived critical sizes are presented for homogeneous mixtures, at theoretical density, of $^{239}\text{PuO}_2\text{-U(0.71)O}_2$ -water in slab, spherical, and cylindrical geometries at the three experimental H/X atomic ratios. These types of data provide the bases for establishing criticality safety control limits.

Critical thicknesses of 10.80 ± 0.11 , 11.56 ± 0.09 , and 14.83 ± 0.60 cm were determined, respectively, for slabs of the 30.0, 14.62, and 7.89 wt% Pu-enriched fuels infinite in two dimensions and fully reflected with 15 cm of Plexiglas. Values of k_{eff} within 8 mk of unity were calculated for these three critical systems using either the diffusion theory code, HFN, or the transport theory code, DTF-IV, with the original GAMTEC-II cross-section data previously used at the Critical Mass Laboratory in correlating plutonium critical experiments with theory. Similar calculations with ENDF/B-II cross-section data yielded k_{eff} values within 12 mk of unity for these three one-dimensional slab assemblies. Except for the more highly moderated 8 wt% Pu-enriched fuel (H/Pu = 659), calculations with ENDF/B-II data resulted in higher k_{eff} values for the critical assemblies than did like calculations using the original GAMTEC-II cross-section library. In the case of the 8 wt% Pu enriched fuel, the computed values for k_{eff} were essentially the same for either of the cross-section sets used.

INTRODUCTION

The operations within a liquid metal fast breeder reactor (LMFBR) industry involve the daily handling of thousands of kilograms of fuel that is highly enriched with plutonium. To assure criticality safety, or prevent nuclear criticality accidents, in such operations, limits will be required on the equipment design and the amount of fuel that may be handled or processed at any one location at any one time. However, these same limits or controls also present the main restriction to plant through-put, which directly affects plant economy. The criticality control limits may dictate operations which are far from optimum economically—the greater the uncertainty in a

knowledge of criticality for a given operation, the more severe the restrictions become. Since an efficient fuel cycle is considered essential to the attainment of a successful LMFBR industry, criticality data are required on plutonium-uranium fuels to provide standards of excellence on criticality control throughout the fuel cycle operations.

Although a major benchmark program is under way to provide the necessary data for reactor core design, the experimental assemblies are limited to fast, heterogeneous systems containing essentially no hydrogenous material. However, the conditions that may be encountered by the fuel external to the reactors (fuel recycle operations) are such as to result in much smaller critical masses for the fuel than within the reactor core,

and to require consideration of thermal- and intermediate-energy systems as well as fast systems. It is estimated that two-thirds of the fuel cycle operating costs for an LMFBR will be derived from fuel fabrication and spent fuel recovery operations, including storage and shipment.¹ Unfortunately, the calculational checks made against integral critical experiments on fast assemblies provide little, if any, assurance that the calculations will produce valid results in a thermal or an intermediate spectrum. A research program is currently under way at the Critical Mass Laboratory to provide the necessary criticality data on mixed-oxide fuels of plutonium and uranium for the specific conditions and configurations which the fuels will encounter outside the reactor core. These data will serve as the basis for establishing criticality control limits for these operations and will provide certain benchmark data for verifying computational methods and cross-section sets (such as ENDF/B cross-section data) used in criticality calculations.

The initial experiments at the Critical Mass Laboratory were conducted with mixed-oxide fuels containing depleted uranium enriched with about 8, 15, and 30 wt% plutonium to cover the enrichment range currently of interest in the LMFBR program. Data from critical experiments with fuel at these three enrichments and at H/X (H:Pu+U)

atomic ratios near optimum for either minimum critical volume or minimum critical mass are presented in this paper. The data are given in two forms: first, as direct experimental data, which can be used as integral benchmark data for checking cross-section sets and calculational models; and second, as theoretical density ²³⁹PuO₂-U(0.71)O₂-water criticality data derived from the experiments with the respective H/X fuel.

EXPERIMENTS

The experiments were performed using the split-table machine, shown in Fig. 1 with the table halves separated and the Plexiglas reflector partially removed to display the fuel core. Each of the fuels consisted of a homogeneous mixture of PuO₂-UO₂-polystyrene in the form of 2- × 2-in. compacts having thicknesses of 2, 1½, and ½ in. Each compact was clad with 6-mil-thick tape (MM&M #471). Nuclide composition and densities are given in Table I for each of the three fuels and for the Plexiglas reflector used in the experiments. In all three fuels the plutonium contained 8 wt% ²⁴⁰Pu and the uranium was depleted to 0.151 wt% ²³⁵U. Particle size distributions for the oxides and the polystyrene are given in Table II.

Inverse multiplication measurements were made on both bare and Plexiglas-reflected parallelepipeds of the 30 wt% Pu fuel and the 14.62 wt% Pu fuel listed in Table I. Measurements on the 7.89 wt% Pu fuel listed in Table I were restricted to Plexiglas-reflected assemblies by the prohibi-

¹Liquid Metal Fast Breeder Reactor Program Plan, Vol. 8, Fuel Recycle, WASH-1108, U.S. Atomic Energy Commission (1968).

TABLE I
Composition and Atom Densities of Experimental Fuel and Reflector Material*

| Nuclide Composition | at./ (b cm) | | | |
|--------------------------------|--|---|--|--------------------------|
| | 426 g Oxide/liter Atomic H/X = 47.4 30.0 wt% Pu ^a | 660 g Oxide/liter Atomic H/X = 30.6 14.62 wt% Pu ^b | 408 g Oxide/liter Atomic H/X = 51.8 7.89 wt% Pu ^c | Reflector |
| ²⁴¹ Am | 3.511 × 10 ⁻⁷ | 4.036 × 10 ⁻⁷ | 1.741 × 10 ⁻⁷ | --- |
| ²³⁹ Pu | 2.578 × 10 ⁻⁴ | 1.954 × 10 ⁻⁴ | 6.528 × 10 ⁻⁵ | --- |
| ²³⁸ Pu | 0.0 | 0.0 | 0.0 | --- |
| ²⁴⁰ Pu | 2.257 × 10 ⁻⁵ | 1.702 × 10 ⁻⁵ | 5.941 × 10 ⁻⁶ | --- |
| ²⁴¹ Pu ^d | 1.756 × 10 ⁻⁶ | 1.211 × 10 ⁻⁶ | 3.481 × 10 ⁻⁷ | --- |
| ²⁴² Pu | 0.0 | 0.0 | 0.0 | --- |
| O | 1.974 × 10 ⁻³ | 3.023 × 10 ⁻³ | 1.830 × 10 ⁻³ | 1.428 × 10 ⁻² |
| ²³⁸ U | 6.604 × 10 ⁻⁴ | 1.252 × 10 ⁻³ | 8.376 × 10 ⁻⁴ | --- |
| ²³⁵ U | 1.008 × 10 ⁻⁵ | 1.904 × 10 ⁻⁶ | 1.285 × 10 ⁻⁶ | --- |
| H | 4.468 × 10 ⁻² | 4.489 × 10 ⁻² | 4.719 × 10 ⁻² | 5.712 × 10 ⁻² |
| C | 4.537 × 10 ⁻² | 4.412 × 10 ⁻² | 4.540 × 10 ⁻² | 3.570 × 10 ⁻² |

*PuO₂, UO₂, and polystyrene each originated from a common source. The accuracy of each nuclide's concentration can be obtained from the variations in the respective isotopic ratios.

^a²⁴¹Am analysis made 5-28-70. Experiments performed February 1970.

^b²⁴¹Am analysis made 5-28-70. Experiments performed June-September 1970.

^c²⁴¹Am analysis made 1-21-71. Experiments performed December 1970-May 1971.

^d13.2-yr half-life used for ²⁴¹Pu decay to ²⁴¹Am.



Fig. 1. Remote split table with faces separated.

TABLE II
Particle Size Distribution in PuO₂-UO₂
Polystyrene Fuels

| Distribution | Particle Diameter, μm | | |
|--------------|----------------------------------|-----------------|-------------|
| | PuO ₂ | UO ₂ | Polystyrene |
| 95% | <20 | <40 | <225 |
| 50% | <5 | <9 | <150 |
| 5% | <0.5 | <3 | <50 |

tively large volume of fuel required for criticality unreflected. The reflected critical assemblies were varied from near-cubic geometry to thin slabs to permit determining, for each of these fuels, both the critical cube size and the critical thickness of a slab infinite in two dimensions. Measurements on the bare assemblies were limited to near-cubic geometry.

EXPERIMENTAL DATA FOR
BENCHMARK TESTING

Experimentally measured critical sizes and masses are given in Tables III, IV, and V for the

TABLE III

Criticality Data for PuO₂-UO₂-Polystyrene Fuel Mixtures

373 g (Pu + U)/liter at 30.0 wt% Pu; H/(Pu + U) = 47.4 atomic

H/Pu = 158; ²⁴⁰Pu content of Pu = 8.0 wt%; ²³⁵U content of U = 0.151 wt%

| Reflector | Critical Dimensions, cm ^a | | | Critical Mass ^a | | Calculated k_{eff} | | | | |
|------------------------|--------------------------------------|--------------|--------------|----------------------------|--------------|----------------------------|-------------------------------|-------------------------------|-------------------------------|----------------------------|
| | | | | | | GAMTEC-11-HFN ^b | GAMTEC-II-DTF-IV ^b | GAMTEC-II-KENO-I ^b | GAMTEC-II-KENO-I ^c | GAMTEC-II-HFN ^c |
| | Length | Width | Height | kg of Pu | kg of U | | | | | |
| Plexiglas | 30.54 ± 0.03 | 30.54 ± 0.03 | 30.89 ± 0.02 | 3.23 ± 0.05 | 7.53 ± 0.12 | --- | --- | 1.011 ± 0.008 | 1.021 ± 0.008 | --- |
| Plexiglas | 35.63 ± 0.04 | 35.63 ± 0.04 | 23.95 ± 0.10 | 3.40 ± 0.05 | 7.94 ± 0.12 | --- | --- | --- | --- | --- |
| Plexiglas | 40.72 ± 0.04 | 40.72 ± 0.04 | 20.22 ± 0.05 | 3.75 ± 0.05 | 8.76 ± 0.13 | --- | --- | --- | --- | --- |
| Plexiglas | 50.90 ± 0.05 | 45.81 ± 0.05 | 17.14 ± 0.07 | 4.48 ± 0.06 | 10.44 ± 0.16 | --- | --- | --- | --- | --- |
| Plexiglas | 61.08 ± 0.06 | 50.90 ± 0.05 | 15.53 ± 0.11 | 5.44 ± 0.08 | 12.69 ± 0.20 | --- | --- | --- | --- | --- |
| Plexiglas | 61.08 ± 0.06 | 55.99 ± 0.06 | 15.16 ± 0.02 | 5.80 ± 0.09 | 13.51 ± 0.21 | --- | --- | --- | --- | --- |
| Plexiglas | 66.17 ± 0.06 | 61.08 ± 0.06 | 14.43 ± 0.10 | 6.53 ± 0.09 | 15.24 ± 0.22 | --- | --- | 1.022 ± 0.007 | --- | --- |
| Plexiglas | 50.90 ± 0.05 | 50.90 ± 0.05 | 16.49 ± 0.04 | 4.78 ± 0.08 | 11.14 ± 0.18 | --- | --- | --- | --- | --- |
| Plexiglas ^d | 30.60 ± 0.02 | 30.60 ± 0.02 | 30.60 ± 0.02 | 3.21 ± 0.05 | 7.49 ± 0.12 | --- | --- | --- | --- | --- |
| Plexiglas ^d | ∞ | ∞ | 10.80 ± 0.11 | --- | --- | 1.006 | 1.008 | --- | --- | 1.012 |
| Bare | 45.81 ± 0.05 | 40.72 ± 0.04 | 37.98 ± 0.06 | 7.93 ± 0.12 | 18.51 ± 0.78 | 0.993 | 0.989 | --- | --- | --- |
| Bare | 40.72 ± 0.04 | 40.72 ± 0.04 | 42.24 ± 0.03 | 7.84 ± 0.11 | 18.30 ± 0.77 | 0.994 | 0.988 | 0.977 ± 0.008 | 1.014 ± 0.006 | --- |
| Bare | 45.81 ± 0.05 | 50.90 ± 0.05 | 32.49 ± 0.02 | 8.48 ± 0.12 | 19.80 ± 0.84 | 0.989 | 0.988 | --- | --- | --- |
| Bare ^d | 41.20 ± 0.05 | 41.20 ± 0.05 | 41.20 ± 0.05 | 7.83 ± 0.11 | 18.28 ± 0.77 | --- | --- | --- | --- | --- |

^aExperimentally determined corrections have been made, accounting for the reactivity effects of the cladding material, the stacking voids, and the structural supports.

^b18-group averaged cross sections using the original GAMTEC-II cross-section library.

^c18-group averaged cross sections using FLANGE-ETOG processed ENDF/B-II data.

^dInfinite slab thickness obtained by extrapolation of data. Cube dimensions obtained by interpolation between critical assemblies.

TABLE IV

Criticality Data for PuO₂-UO₂-Polystyrene Fuel Mixtures

580 g (Pu + U)/liter at 14.62 wt% Pu; H/(Pu + U) = 30.6 atomic
 H/Pu = 210; ²⁴⁰Pu content of Pu = 8.0 wt%; ²³⁵U content of U = 0.151 wt%

| Reflector | Critical Dimensions, cm ^a | | | Critical Mass ^a | | Calculated k_{eff} | | | | |
|------------------------|--------------------------------------|--------------|--------------|----------------------------|--------------|--------------------------------|-----------------------------------|-----------------------------------|-----------------------------------|--------------------------------|
| | Length | Width | Height | kg of Pu | kg of U | GAMTEC-II- HFN ^b | GAMTEC-II- DTF-IV ^b | GAMTEC-II- KENO-I ^b | GAMTEC-II- KENO-I ^c | GAMTEC-II- HFN ^c |
| | | | | | | | | | | |
| Plexiglas | 30.54 ± 0.03 | 40.72 ± 0.04 | 29.81 ± 0.15 | 3.14 ± 0.04 | 18.35 ± 0.35 | --- | --- | 1.007 ± 0.008 | 1.033 ± 0.008 | --- |
| Plexiglas | 40.72 ± 0.04 | 40.72 ± 0.04 | 23.84 ± 0.10 | 3.35 ± 0.04 | 19.57 ± 0.37 | --- | --- | --- | --- | --- |
| Plexiglas | 45.81 ± 0.04 | 50.90 ± 0.05 | 19.82 ± 0.11 | 3.92 ± 0.05 | 22.89 ± 0.44 | --- | --- | --- | --- | --- |
| Plexiglas | 50.90 ± 0.05 | 50.90 ± 0.05 | 18.92 ± 0.09 | 4.16 ± 0.05 | 24.28 ± 0.46 | --- | --- | --- | --- | --- |
| Plexiglas | 61.08 ± 0.06 | 50.90 ± 0.05 | 17.72 ± 0.09 | 4.67 ± 0.06 | 27.28 ± 0.52 | --- | --- | --- | --- | --- |
| Plexiglas | 61.08 ± 0.06 | 61.08 ± 0.06 | 16.63 ± 0.09 | 5.26 ± 0.06 | 30.73 ± 0.59 | --- | --- | 1.008 ± 0.008 | --- | --- |
| Plexiglas ^d | 33.30 ± 0.17 | 33.30 ± 0.17 | 33.30 ± 0.17 | 3.13 ± 0.05 | 18.28 ± 0.40 | --- | --- | --- | --- | --- |
| Plexiglas ^d | ∞ | ∞ | 11.56 ± 0.09 | --- | --- | 0.999 | 1.002 | --- | --- | 1.007 |
| Bare | 40.72 ± 0.04 | 40.76 ± 0.17 | 52.39 ± 0.07 | 7.37 ± 0.09 | 43.06 ± 0.82 | 1.013 | 1.005 | --- | --- | --- |
| Bare | 40.72 ± 0.04 | 45.86 ± 0.19 | 45.10 ± 0.06 | 7.14 ± 0.08 | 41.70 ± 0.79 | 1.012 | 1.005 | 0.995 ± 0.007 | 1.032 ± 0.007 | --- |
| Bare | 50.90 ± 0.005 | 45.86 ± 0.19 | 36.99 ± 0.05 | 7.32 ± 0.08 | 42.75 ± 0.81 | 1.008 | 1.003 | --- | --- | --- |
| Bare ^d | 43.78 ± 0.07 | 43.78 ± 0.07 | 43.78 ± 0.07 | 7.12 ± 0.08 | 41.55 ± 0.80 | --- | --- | --- | --- | --- |

^aExperimentally determined corrections have been made, accounting for the reactivity effects of the cladding material, the stacking voids, and the structural supports.

^b18-group averaged cross sections using the original GAMTEC-II cross-section library.

^c18-group averaged cross sections using FLANGE-ETOG processed ENDF/B-II data.

^dInfinite slab thickness obtained by extrapolation of data. Cube dimensions obtained by interpolation between critical assemblies.

TABLE V
Criticality Data for PuO₂-UO₂-Polystyrene Fuel Mixtures
360 g(Pu + U)/liter at 7.89 wt% Pu; H/(Pu + U) = 51.8 atomic H/Pu = 659; ²⁴⁰Pu content of Pu = 8.0 wt%; ²³⁵U content of U = 0.151 wt%

| Reflector | Critical Dimensions, cm ^a | | | Critical Mass ^a | | Calculated k_{eff} | | | | |
|------------------------|--------------------------------------|--------------|---------------------------|----------------------------|--------------|-------------------------------|----------------------------------|----------------------------------|----------------------------------|--------------------------------|
| | Length | Width | Height | kg of Pu | kg of U | GAMTEC-II HFN ^b | GAMTEC-II DTF-IV ^b | GAMTEC-II KENO-I ^b | GAMTEC-II KENO-I ^c | GAMTEC-II- HFN ^c |
| | | | | | | | | | | |
| Plexiglas | 40.72 ± 0.04 | 45.72 ± 0.09 | 32.89 ± 0.12 | 1.74 ± 0.01 | 20.29 ± 0.22 | --- | --- | --- | --- | --- |
| Plexiglas | 50.90 ± 0.05 | 50.80 ± 0.10 | 26.40 ± 0.10 | 1.94 ± 0.02 | 22.63 ± 0.25 | --- | --- | --- | --- | --- |
| Plexiglas | 61.08 ± 0.06 | 60.96 ± 0.12 | 22.66 ± 0.08 | 2.39 ± 0.02 | 27.88 ± 0.31 | --- | --- | --- | --- | --- |
| Plexiglas | 61.08 ± 0.06 | 66.04 ± 0.13 | 22.09 ± 0.18 | 2.53 ± 0.03 | 29.53 ± 0.39 | --- | --- | --- | --- | --- |
| Plexiglas | 61.08 ± 0.06 | 55.88 ± 0.11 | 23.22 ± 0.08 | 2.25 ± 0.02 | 26.26 ± 0.28 | --- | --- | 1.029 ± 0.007 | 1.034 ± 0.008 | --- |
| Plexiglas | 61.08 ± 0.06 | 50.80 ± 0.10 | 24.37 ± 0.09 ^d | 2.15 ± 0.02 | 25.06 ± 0.28 | --- | --- | 1.021 ± 0.007 | 1.008 ± 0.008 | --- |
| Plexiglas | 40.72 ± 0.05 | 40.64 ± 0.08 | 36.42 ± 0.13 | 1.71 ± 0.01 | 19.97 ± 0.22 | --- | --- | 1.032 ± 0.007 | 1.027 ± 0.007 | --- |
| Plexiglas ^e | 39.12 ± 0.28 | 39.12 ± 0.28 | 39.12 ± 0.28 | 1.70 ± 0.01 | 19.84 ± 0.32 | --- | --- | --- | --- | --- |
| Plexiglas ^e | ∞ | ∞ | 14.83 ± 0.60 | --- | --- | 0.993 | 0.998 | --- | --- | 0.991 |

^a Experimentally determined corrections have been made, accounting for the reactivity effects of the cladding material and the stacking voids.

^b 18-group averaged cross sections using the original GAMTEC-II cross-section library.

^c 18-group averaged cross sections using FLANGE-ETOG processed ENDF/B-II data.

^d Average of two experiments.

^e Infinite slab thickness obtained by extrapolation of data. Cube dimensions obtained by interpolation between critical assemblies.

three PuO₂-UO₂-polystyrene fuels containing 30.0, 14.62, and 7.89 wt% Pu, respectively, in the plutonium-uranium. The critical sizes and masses given in these three tables are for solid assemblies of fuel only. Experimentally determined corrections have been applied in each case to account for the effects of the cladding material and the presence of voids in the assembly of stacked blocks. These corrections were determined by observing the change in critical mass with varying thicknesses of cladding material, as indicated typically in Fig. 2 for a reflected assembly of each of the three fuels. For the bare assemblies, a small additional correction was also required to account for the reactivity effect of the structural supports. This correction amounted to an increase of only 0.05% on the critical mass of each bare assembly and was determined by replacement type measurements. The error limits quoted in these three tables, and elsewhere in this paper, are one-sigma limits.

Some critical sizes and masses obtained by interpolation between, or extrapolation of, the experimental data also are shown in Tables III, IV, and V. The critical cube data were obtained by interpolation between the two critical assemblies nearest a critical cube of the particular fuel. The interpolation in each case was made by searching for the critical assembly whose cross section was the square of its height (Figs. 3, 4, and 5) and by bearing in mind that, in rectangular geometry, the

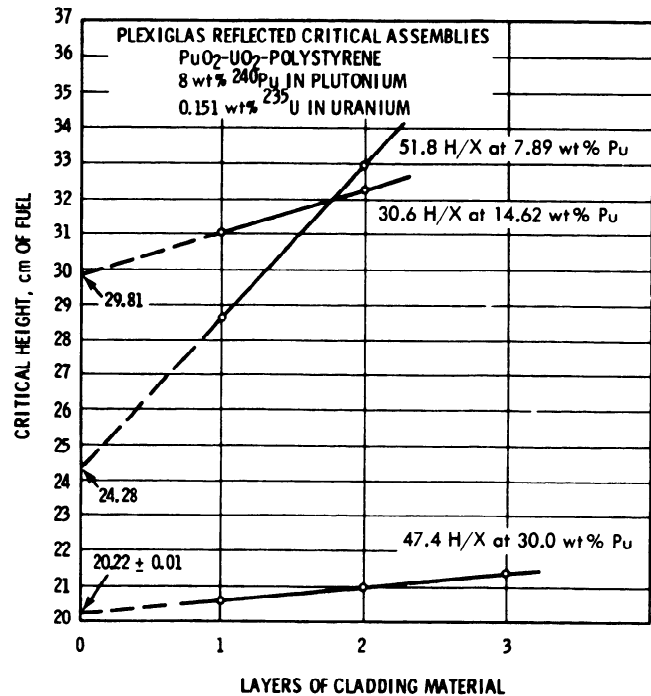


Fig. 2. Combined effect of voids and fuel cladding on the critical height of reflected assemblies.

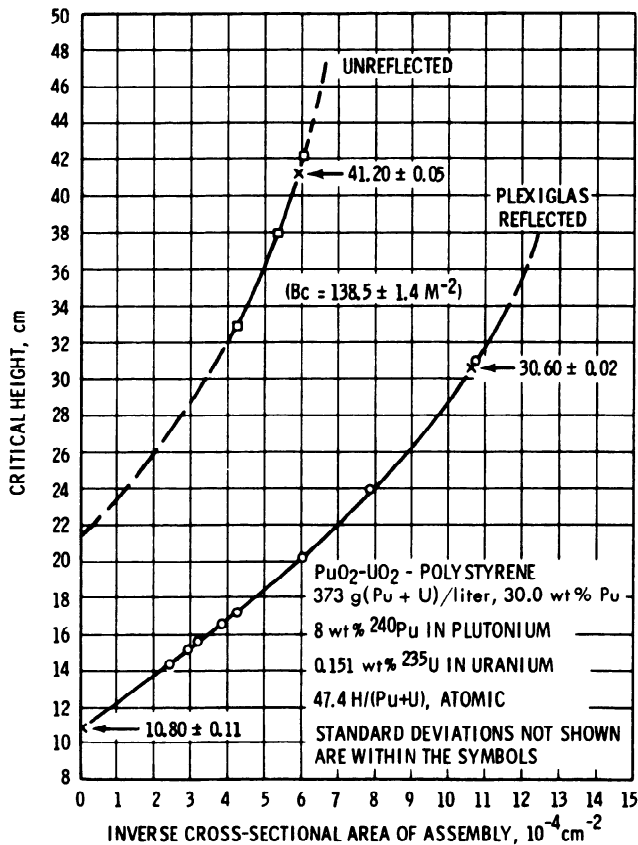


Fig. 3. Measured critical height.

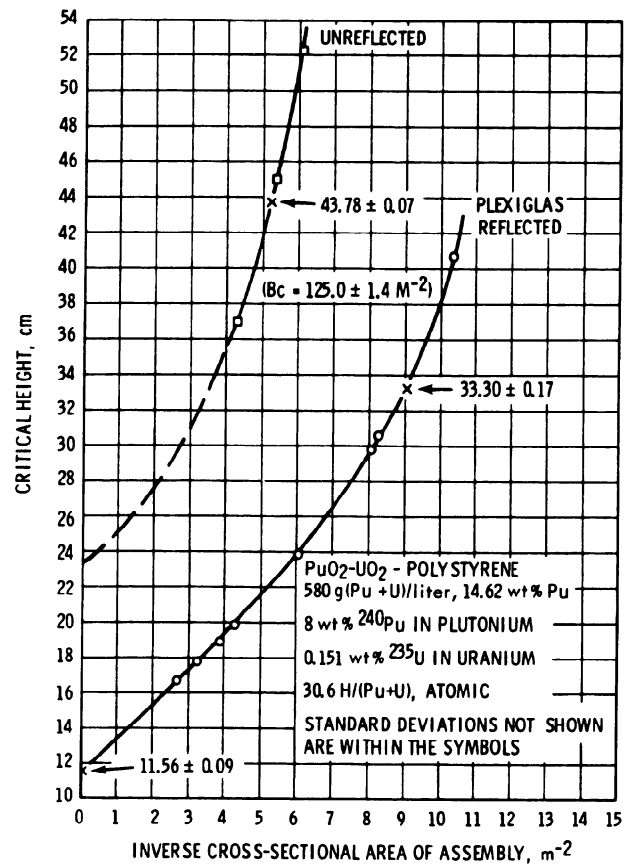


Fig. 4. Measured critical height.

cube should contain the smallest critical mass. The error limits reported for each cube are arbitrarily set such that a linear interpolation between the two critical assemblies on either side of the respective cube is within these error limits. An extrapolated critical thickness for a reflected slab, infinite in two dimensions, is also shown in each of the Tables III, IV, and V for the respective fuel. For the 30.0 and 14.62 wt% Pu-enriched fuels, the reflected infinite slab critical thickness was obtained by a linear extrapolation of the critical heights of finite systems of thin slabs as their inverse cross-sectional area approached zero. Although some curvature is probably still present as each system approaches the infinite condition, it is small and would result in a slightly larger critical slab thickness for each fuel. These thicknesses are believed to be within the error limits quoted, since, as noted later, the critical buckling for each of these fuels and the respective reflector savings result in a critical thickness for each fuel that is within these limits.

For the 7.89 wt% Pu-enriched fuel, an abnormal amount of scatter was observed in the measured critical heights. This was due, in part, to the large reactivity effect of the stacking voids and

cladding material (about 15 wt% compared to less than 4 wt% in previous fuels) and in part to an insufficient amount of fuel for obtaining the best combination of fuel blocks in some of the critical approaches. Consequently, the critical thickness of a slab of this fuel, infinite in two directions, could not be obtained as accurately from a linear extrapolation as was done with the 30.0 and 14.62 wt% Pu-enriched fuels. However, the linear extrapolation should provide a lower bound for the infinite slab thickness, and the thickness obtained from the critical buckling and reflector savings, which will be covered later, should provide an upper bound. The critical thickness of 14.83 cm for a reflected infinite slab given in Table V and Fig. 5 is the average of these two bounds, and the quoted standard deviation of ± 0.6 cm is the difference between the 14.83 cm and the two bounds.

The critical bucklings, referred to previously, for the 30.0 and 14.62 wt% Pu-enriched fuels were determined from the bare critical assemblies of these fuels by calculating an extrapolation distance for a bare cube of each fuel and then applying these extrapolation distances to the bare critical dimensions measured for each of the respective fuels. Each extrapolation distance was calculated

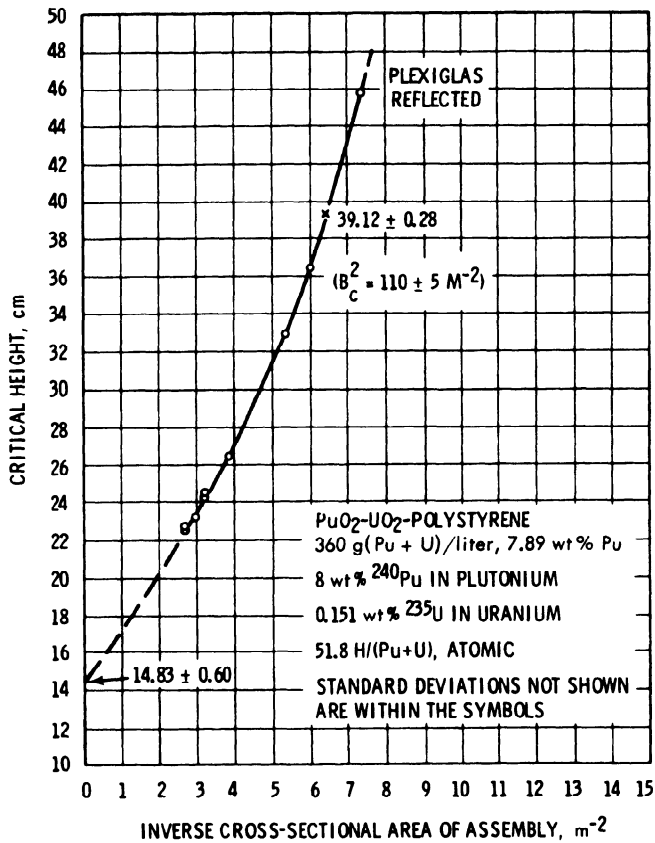


Fig. 5. Measured critical height.

using 18-energy group averaged constants from GAMTEC-II² as input to the diffusion code HFN³ to calculate the difference in the critical height of a near-cubic assembly with the neutron flux vanishing at the physical and extrapolated boundaries. The buckling values obtained for the six bare critical assemblies measured are shown in Table VI.

For the three bare assemblies of 30.0 wt% Pu-enriched fuel, an extrapolation distance of 2.56 cm was calculated. This extrapolation distance, when used with the critical dimensions of each assembly, yields a constant geometrical buckling of 138.46 m⁻² for the three assemblies, in that all three bucklings are within one standard deviation of 1.39 m⁻² of each other. The standard deviation was arrived at by propagation of errors using the quoted standard deviations on the measured dimensions and an arbitrary standard deviation on the calculated extrapolation distance that would reproduce the maximum observed variations in the three geometrical bucklings. In like manner,

²L. L. CARTER, C. R. RICHEY, and C. E. HUGHEY, "GAMTEC-II: A Code for Generating Consistent Multi-group Constants Utilized in Diffusion and Transport Theory Calculations," BNWL-35, Pacific Northwest Laboratory (1965).

³J. R. LILLEY, "Computer Code HFN—Multigroup, Multiregion Neutron Diffusion Theory in One Space Dimension," HW-71545, General Electric Company (1961).

TABLE VI
Critical Bucklings for Unreflected PuO₂-UO₂-Polystyrene Critical Assemblies

373 g (Pu + U)/liter at 30.0 wt% Pu; H/(Pu + U) = 47.4 atomic
H/Pu = 158.2; ²⁴⁰Pu content of Pu = 8.0 wt%; ²³⁵U content of U = 0.151 wt%

| Critical Dimensions, cm | | | B _g ² , m ⁻² (λ = 2.56 ± 0.08 cm) ^a | Calculated ^b B _m ⁻² m ⁻² |
|--|--------------|--------------|--|---|
| Width | Length | Height | | |
| 45.81 ± 0.05 | 40.72 ± 0.04 | 37.98 ± 0.06 | 138.16 ± 1.34 | --- |
| 40.72 ± 0.04 | 40.72 ± 0.04 | 42.24 ± 0.03 | 137.94 ± 1.28 | --- |
| 45.81 ± 0.05 | 50.90 ± 0.04 | 32.49 ± 0.03 | 139.27 ± 1.54 | --- |
| Average | | | 138.46 ± 1.39 | 133.94 |
| 580 g (Pu + U)/liter at 14.62 wt% Pu; H/(Pu + U) = 30.6 atomic H/Pu = 210.1; ²⁴⁰ Pu content of Pu = 8.0 wt%; ²³⁵ U content of U = 0.151 wt% | | | | |
| | | | (λ = 2.49 ± 0.07 cm) ^a | |
| 40.76 ± 0.17 | 40.72 ± 0.04 | 52.39 ± 0.07 | 124.42 ± 1.47 | --- |
| 45.86 ± 0.19 | 40.72 ± 0.04 | 45.10 ± 0.06 | 124.79 ± 1.36 | --- |
| 45.86 ± 0.19 | 50.90 ± 0.05 | 36.99 ± 0.05 | 125.82 ± 1.43 | --- |
| Average | | | 125.01 ± 1.43 | 127.07 |

^aOne-half the difference between the critical heights calculated with the neutron flux going to zero at the physical and extrapolated boundaries.

^bEighteen-group GAMTEC-II calculations using the original GAMTEC-II cross-section library.²

an extrapolation distance of 2.49 cm was calculated for the 14.62 wt% Pu-enriched fuel and yielded a constant geometrical buckling of $125.01 \pm 1.43 \text{ cm}^{-2}$ for the three assemblies.

Although various processing techniques are currently being evaluated for reducing ENDF cross sections to a usable format, ENDF cross sections were not used in calculating the extrapolation distances. However, as shown in Tables III and IV, the cross sections used (original GAMTEC-II cross-section library) were capable of computing the six unreflected critical assemblies to within 13 mk. Although the ENDF cross sections should not affect the calculated values for the extrapolation distances and, thus, the buckling calculated for a given system, there are some indications that the various cross-section processing codes insert their own bias.⁴ However, since buckling conversion tends to be self-compensating, the effects on the results reported in this paper are small and are within the error limits quoted.

Since the bare critical size was not measured for a 7.89 wt% Pu-enriched system, calculations had to be relied upon entirely to obtain a critical buckling for this fuel. For the 30.0 and the 14.62 wt% Pu-enriched fuels the respective GAMTEC-II calculated material bucklings were within about 4.0 m^{-2} of the critical bucklings determined for these fuels (see Table VI). Consequently, a GAMTEC-II calculated buckling of 111.0 m^{-2} and a standard deviation of 5.0 m^{-2} was assumed for the 7.89 wt% enriched fuel.

Extrapolation distances for each of the reflected assemblies were determined by equating the critical buckling of each fuel to the measured physical size of the respective critical assemblies. These extrapolation distances are plotted in Fig. 6 as an inverse function of the cross-sectional area of the respective assemblies. A linear extrapolation of these data was made to obtain the extrapolation distance for a slab of each fuel infinite in two directions. The reflected extrapolation distances obtained in this manner for an infinite slab are consistent with the infinite slab thicknesses obtained independently in Figs. 3, 4, and 5 (except that the slab thickness shown for the 7.89 wt% Pu-enriched fuel is not completely independent, as discussed before). These extrapolation distances and slab thicknesses will yield the critical buckling of the respective fuel within the error limits quoted. As in past critical experiments of this type, the extrapolation distances, obtained in this manner, appear to be a more sensitive indicator of any scatter in the experimental

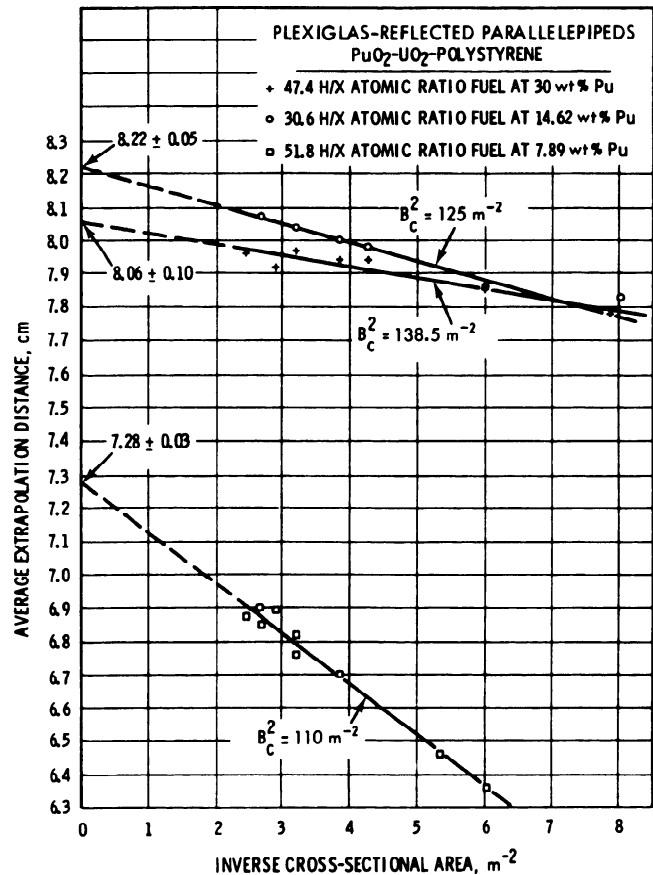


Fig. 6. Variation in average extrapolation distance with geometry.

data than do the corresponding critical dimensions. It was for this reason that the extrapolation distance of 7.28 cm thus obtained for the 7.89 wt% Pu-enriched fuel (where some scatter was observed in the critical heights as the infinite case was approached) was given some consideration, as mentioned before, in obtaining a critical thickness for a reflected slab of this fuel infinite in two directions.

DERIVED DATA FOR NUCLEAR CRITICALITY SAFETY

To facilitate the use of the experimental data in establishing criticality safety limits, buckling conversions were employed to obtain both bare and Plexiglas-reflected sizes for each of the fuels in spherical, cylindrical, and slab geometries. Each of these values was then computationally corrected for density, carbon, and oxygen effects to obtain critical sizes at the respective H/X atomic ratios for theoretical density $^{239}\text{PuO}_2\text{-U}(0.71)\text{O}_2\text{-H}_2\text{O}$ in both bare and water-reflected spherical, cylindrical, and slab geometries. These values are tabulated in Table VII.

⁴L. E. HANSEN and E. D. CLAYTON, *Trans. Am. Nucl. Soc.*, **15**, 1 (1972).

TABLE VII
Critical Dimensions in Spherical, Cylindrical, and Slab Geometries

| Geometry | Critical Dimensions, cm ^a | | | | | |
|---|--------------------------------------|--------------|--------------|--------------|-------------------|--------------|
| | Infinite Slab | | Sphere | | Infinite Cylinder | |
| | Bare | Reflected | Bare | Reflected | Bare | Reflected |
| Critical Assembly 47.4 H/X Atomic Ratio at 30.0 wt% Pu | | | | | | |
| PuO ₂ -UO ₂ -polystyrene ^b ²³⁹ PuO ₂ -U(0.72)O ₂ -water ^c | 21.70 ± 0.15 | 10.80 ± 0.11 | 24.20 ± 0.14 | 18.50 ± 0.27 | 17.94 ± 0.11 | 12.31 ± 0.10 |
| | 14.95 ± 0.10 | 7.06 ± 0.07 | 17.05 ± 0.10 | 13.16 ± 0.13 | 12.18 ± 0.07 | 8.60 ± 0.07 |
| 30.6 H/X Atomic Ratio at 14.62 wt% Pu | | | | | | |
| PuO ₂ -UO ₂ -polystyrene ^b ²³⁹ PuO ₂ -U(0.72)O ₂ -water ^c | 23.22 ± 0.21 | 11.56 ± 0.09 | 25.67 ± 0.17 | 19.72 ± 0.21 | 19.08 ± 0.14 | 13.19 ± 0.12 |
| | 8.20 ± 0.08 | 7.86 ± 0.06 | 18.52 ± 0.12 | 14.41 ± 0.15 | 13.57 ± 0.10 | 9.48 ± 0.09 |
| 51.8 H/X Atomic Ratio at 7.89 wt% Pu | | | | | | |
| PuO ₂ -UO ₂ -polystyrene ^b ²³⁹ PuO ₂ -U(0.72)O ₂ -water ^c | 25.31 ± 0.20 | 14.83 ± 0.60 | 27.64 ± 0.10 | 22.56 ± 0.10 | 20.62 ± 0.10 | 15.58 ± 0.10 |
| | 18.61 ± 0.15 | 10.48 ± 0.42 | 20.62 ± 0.07 | 16.91 ± 0.07 | 15.30 ± 0.12 | 11.50 ± 0.07 |

^aCritical thickness of slabs infinite in two directions and critical radii of spheres and infinitely long cylinders.

^bDensity and isotopic concentrations of experimental fuel as given in Table I, full Plexiglas reflection where applicable.

^cTheoretical density oxide-water, full water reflection where applicable; H/X = 47.4, 600 g oxide/liter; H/X = 30.6, 900 g oxide/liter; H/X = 51.8, 549 g oxide/liter.

The bare and water-reflected spherical critical radii and masses are compared in Figs. 7 through 10 with previously reported⁹ sets of curves calculated for use as guides in establishing nuclear criticality safety limits. As can be seen in these figures, the critical sizes and masses derived from the experimental data agree quite well with the calculated curves in the concentration region between about 500 and 1000 g oxide/liter and over the entire uranium enrichment range above 8%.

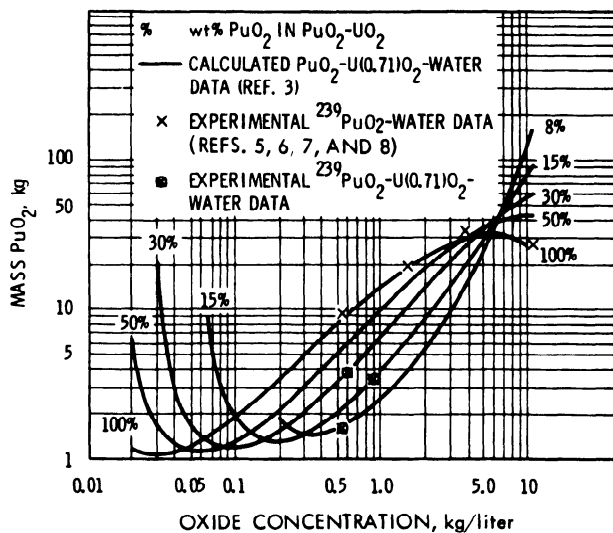


Fig. 7. Unreflected spherical critical mass—²³⁹PuO₂-U(0.71)O₂-water mixtures.

The curves shown in Figs. 7 through 10 were generated⁹ by Hansen using 18-group GEMTEC-II averaged cross sections from the original GAMTEC-II library¹ in the one-dimensional neutron transport theory code, DTF-IV.¹⁰ Values are shown in Tables III, IV, and V for those experimental critical assemblies that lend themselves to this calculational technique. For comparison purposes, and for extending the theory-experiment correlations to the reflected, finite, critical assemblies, some calculated values using the Monte Carlo code, KENO-I¹¹ with 18-group GAMTEC-II averaged cross sections are also shown in these three tables. In each case com-

⁵C. R. RICHEY, J. D. WHITE, E. D. CLAYTON, and R. C. LLOYD, *Nucl. Sci. Eng.*, **23**, 150 (1965).

⁶S. R. BIERMAN, L. E. HANSEN, R. C. LLOYD, and E. D. CLAYTON, *Nucl. Appl.*, **6**, 23 (1969).

⁷S. R. BIERMAN and E. D. CLAYTON, *Nucl. Technol.*, **11**, 185 (1971).

⁸S. R. BIERMAN, E. D. CLAYTON, and L. E. HANSEN, *Nucl. Technol.*, **15**, 5 (1972).

⁹L. E. HANSEN, S. R. BIERMAN, and E. D. CLAYTON, "Criticality of Mixed PuO₂-UO₂ Systems," Reactor Physics Quarterly Report, BNWL-1150, p. 5.6, Pacific Northwest Laboratory (1969).

¹⁰K. D. LATHROP, "DTF-IV—A Fortran-IV Program for Solving the Multigroup Transport Equation With Anisotropic Scattering," LA-3373, Los Alamos Scientific Laboratory (1965).

¹¹G. E. WHITESIDES and N. F. CROSS, "KENO—A Multigroup Monte Carlo Program," CTC-5, Union Carbide Corporation (1969).

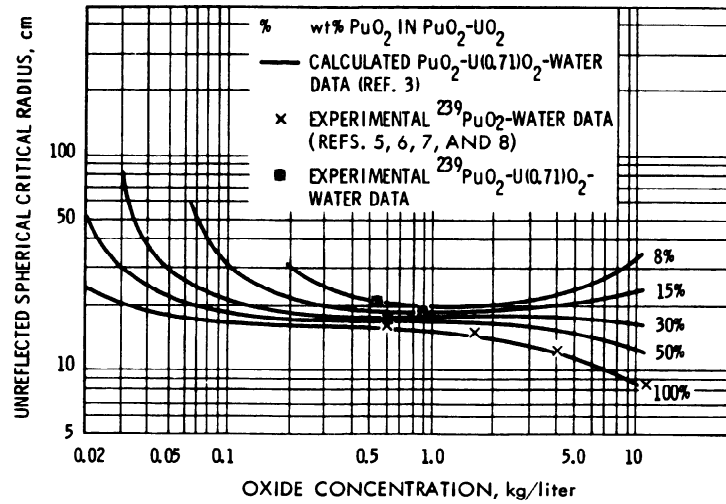


Fig. 8. Unreflected spherical critical radius— $^{239}\text{PuO}_2\text{-U(0.71)O}_2\text{-water}$.

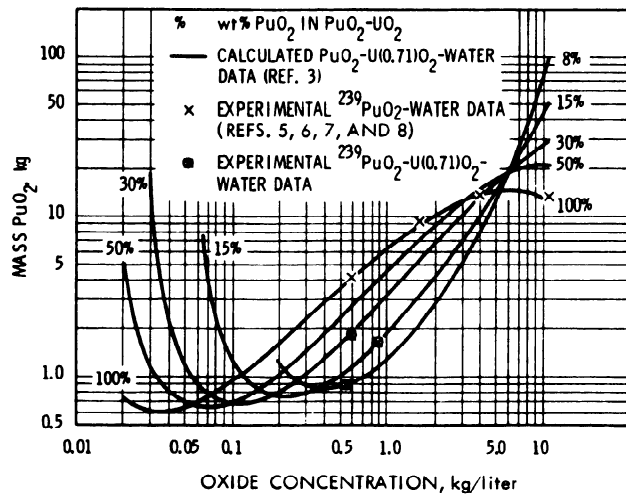


Fig. 9. Water-reflected spherical critical mass— $^{239}\text{PuO}_2\text{-U(0.71)O}_2\text{-water}$.

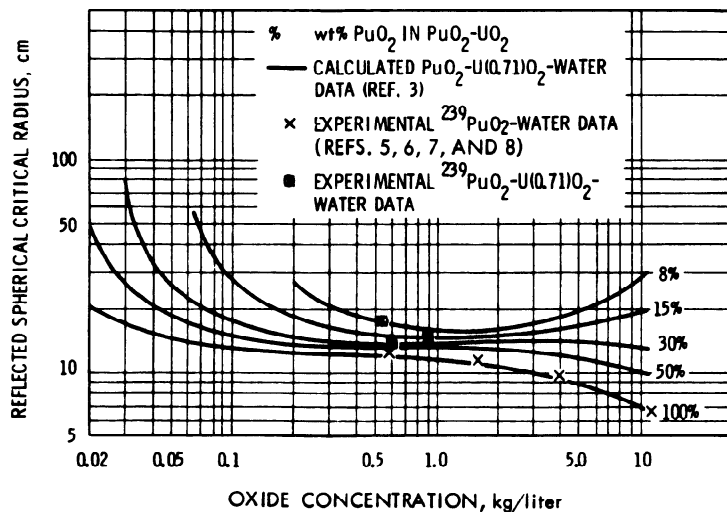


Fig. 10. Water-reflected spherical critical radius— $^{239}\text{PuO}_2\text{-U(0.71)O}_2\text{-water}$.

pared, the GAMTEC-KENO calculation yielded a k_{eff} value about 10 mk lower than the comparable GAMTEC-DTF calculation. For the reflected critical assemblies checked, the GAMTEC-KENO-calculated k_{eff} values were consistently greater than unity by about 10 to 40 mk.

Also shown in Tables III, IV, and V, for comparison, are k_{eff} values for a few of the critical assemblies using 18-group GAMTEC-II ENDF/B-II cross sections. A more thorough testing and evaluation of the cross-section data with these and other previously reported critical experiments is the subject of a paper⁴ currently being prepared for publication. Briefly, however, the 18-group averaged cross-section data were obtained from the ENDF/B-II library by using the FLANGE code¹² to process the thermal data and the ETOG code¹³ to process the epithermal data for broad group averaging in GAMTEC-II. Except for the 7.89 wt% Pu-enriched fuel, KENO-I-calculated k_{eff} values using these cross-section data were slightly higher than comparable values obtained from the GAMTEC-KENO calculations with the original GAMTEC-II cross sections. For the 7.89 wt% Pu-enriched fuel, which had the lowest concentration of Pu, essentially the same KENO-I-calculated k_{eff} values were obtained with either set of cross-section data.

The KENO-I calculated k_{eff} values for the Plexiglas-reflected critical assemblies were consistent with the k_{eff} values obtained for the bare critical assemblies. Consequently, the ENDF/B-II cross sections generated for the Plexiglas are satisfactory. This is further confirmed by the good agreement obtained between the results of one-dimensional diffusion theory calculations (computer code HFN), shown in Tables III, IV, and V, and the experimentally determined critical thicknesses of Plexiglas-reflected slabs of each of these three fuels infinite in two directions.

CONCLUSIONS

The results of the critical experiments reported in this paper provide the initial experimental data on critical masses and sizes of homogeneous mixtures of PuO₂-UO₂ and include data points in the 8 to 30 wt% Pu enrichment range that is currently of interest in the LMFBR program. The data for the 7.89 wt% Pu-enriched fuel

(H/Pu = 659) are very near optimum moderation with respect to mass and thus provide a data check point on the minimum critical mass of mixed oxides at the 8 wt% enrichment level. The data from the 14.62 wt% Pu-enriched fuel (H/Pu = 210) provide a check point at near minimum critical volume in the intermediate enrichment region. The data from the 30.0 wt% Pu-enriched fuel is in the oxide concentration range of nearly constant critical volume and thus provide a check for calculations over a very wide range of concentrations. The calculations reported in this paper indicate that this range of constant volume may exist for all 30.0 wt% Pu-enriched oxide concentrations above about 200 g/liter, except for a slight decrease as the theoretical oxide density is approached. Data in this area (3 H/X) are currently being obtained.

Calculated k_{eff} values, at all three enrichments, are in general agreement with the observed critical sizes; however, except for the 8 wt% Pu enriched fuel, calculated values based on ENDF/B-II data result in slightly higher values of k_{eff} than do the same calculations based on the original GAMTEC-II cross section data previously used at the Hanford Critical Mass Laboratory for evaluating plutonium-fueled critical experiments. It should be borne in mind that in all three cases the assemblies were relatively well moderated, as the H/Pu ratios were in the range between 158 and 659. It is to be expected that the computed values may agree less well with experimental data on more highly undermoderated systems where resonance absorption becomes more significant. For the more thermalized 8 wt% fuel, good agreement was obtained between experiments, both sets of cross-section data, and calculational methods.

A comparison between the data derived from these critical experiments and curves generated by Chalmers^{14,15} using the Monte Carlo code GEM-III,¹⁶ will show general agreement. His reported values for the reflected systems, however, are slightly nonconservative, with respect to criticality safety, whereas the bare systems tend to be slightly conservative.

ACKNOWLEDGMENT

This paper is based on work performed under Contract No. AT(45-1)-1830 between the U.S. Atomic Energy Commission and Battelle Memorial Institute.

¹²H. C. HONECK and D. R. FINCH, "FLANGE-II (Version 71-1): A Code to Process Thermal Neutron Data From an ENDF/B Tape," DP-1278 (ENDF-152), Savannah River Laboratory (1971).

¹³D. E. KUSNER, R. A. DANIELS, and S. KELLMAN, "ETOG-I: A FORTRAN-IV Program to Process Data from the ENDF/B File to the MUFT, GAM, and ANISN Formats," WCAP-3845-1 (ENDF-114), Westinghouse Electric Corporation (1969).

¹⁴J. H. CHALMERS, "Criticality Parameters for Mixtures of Plutonium Oxide, Uranium Oxide and Water," *Criticality Control of Fissile Material*, p. 3, International Atomic Energy Agency, Vienna (1966).

¹⁵J. H. CHALMERS, *Trans. Am. Nucl. Soc.*, **11**, 687 (1968).

¹⁶P. J. HEMMINGS, "The Gem Code," AHSB (S) R 105, United Kingdom Atomic Energy Authority (1967).